

Phases in optical lattices vs. Coulomb frustrated HTc cuprates

H. Heiselberg

*Univ. of S. Denmark, Campusvej 55, DK-5230 Odense M, Denmark**

Fermionic atoms in 2D optical lattices and electrons in HTc cuprates may both be described by the Hubbard model. However, if Coulomb frustration is responsible for the striped phases in 2D cuprates the phase diagrams will differ markedly. Two representative scenarios are described by a simple stripe model without phase separation and a mean field model with phase separation in the absence of Coulomb frustration. When Coulomb frustrated both models display antiferromagnetism (AF) and stripe phases with d-wave superfluidity, whereas neutral atoms in optical lattices will only do so in the stripe model. Radii and densities of the various phases in harmonically confined optical lattices are calculated for the two models and have very different Mott plateaus and density discontinuities. Observation of antiferromagnetic, stripe and superfluid phases in density and momentum distributions and correlations from time-of-flight experiments is discussed.

PACS numbers: 03.75.Ss, 03.75.Lm, 05.30.Fk, 74.25.Ha, 74.72.-h

I. INTRODUCTION

Ultra-cold atomic Fermi-gases present a new opportunity to study strongly correlated quantum many-particle systems. Optical lattices provide a periodical lattice potential in which the atoms are described by the tight-binding approximation, which enables access to the Hubbard model with interactions tuned by Feshbach resonances. Most importantly we gain direct observation into many controversial issues in strongly correlated high temperature (HTc) superconductors in a controllable way where interactions, densities, temperatures, etc., can be tuned. Recent experiments with optical lattices have measured momentum distributions and correlations, and have found superfluid phases of Bose and Fermi atoms [1, 2, 3], Mott insulators [4], and band insulators [5, 6].

HTc cuprates, however, suffer long range Coulomb repulsion between doped electrons or holes (if localized) whereas neutral atoms in optical lattices are not likewise frustrated. Coulomb frustration inhibits phase separation and may also be responsible for stripe formation in cuprates which again affects d-wave superconductivity (dSC). By studying the phases in optical lattices we can directly observe whether phase separation, stripes and dSC occur in the Hubbard model without Coulomb frustration for general density, temperature, interaction strengths, etc.

Many models have been applied for investigating HTc such as the 2D Hubbard and t-J Hamiltonians in different approximate versions with very different results (see [24] and references therein). Extending with next-nearest neighbor hopping and interactions or long-range Coulomb interactions further complicates the problem. Early Hubbard mean field (MF) calculations predicted

phase separation between an antiferromagnetic (AF) phase with density $n = 1$ and a paramagnetic phase for $U \lesssim 7t$ or a ferromagnetic phase for $U \gtrsim 7t$ [7]. Phase separation (PS) in the Hubbard model and the closely related t-J model is still controversial despite intense investigations. In the t-J model PS is found for large J/t but for the more realistic smaller values of J/t the field is divided. In the Hubbard model without next-nearest neighbor interactions ($t' = 0$) exact diagonalization [8] and Monte Carlo results [9] find PS whereas dynamical mean field [10] and variational cluster perturbation theory [11] do not. In dynamical cluster approximations PS is found for finite t' [12].

A MF ground state with stripes was found by Zaanen and Gunnarson [13]. These stripes have a hole density of one per site whereas density matrix renormalization group calculations [14] find a stripe density of 1/2 in accordance with experiments [15]. However, Green's function Monte Carlo calculations [16] find only weak signs of stripes. Various cellular dynamical MF [17] and cluster calculations [18] find competing antiferromagnetic and dSC phases. The long range Coulomb forces in cuprates suppress phase separation, possibly leading to mixed phases with short range density fluctuations such as stripes [20]. The atoms in optical lattices are electrically neutral and the two phases of different densities are therefore not forced to mix by Coulomb forces to e.g. a stripe phase but can remain in separate bulk phases.

The many different results indicate that the ground state is delicately balanced between nearly degenerate phases. Slight approximations or changes in hopping and interaction parameters can change the ground state phase dramatically. Thus, two decades after the discovery of HTc, the ground state and the mechanism of pairing remains undetermined in cuprates as well as Hubbard and t-J models.

The purpose of this work is rather to study qualitative differences in confined optical lattices from simple cal-

*Electronic address: heiselberg@mil.dk

culations for the 2D Hubbard model in which Coulomb frustration play a central or no role for inhibiting phase separation, stripe formation and HTc. To this purpose we specifically investigate in section II two simple representative models with and without PS, their different density distributions and phases. We investigate the effects of Coulomb frustration in section III and show that it is difficult to distinguish the two models in HTc materials because phase separation is inhibited and stripe phases appear in both cases. Likewise dSC appears in the stripe phases as discussed in section IV. Yet in confined optical lattices as described in section V, the absence of Coulomb frustration leads to very different phases, density and momentum distributions and correlations for the two models.

II. EQUATION OF STATES FOR THE 2D HUBBARD MODEL

In the tight binding approximation spin 1/2 fermions are described by the Hubbard model [21]

$$H = -t \sum_{\langle ij \rangle \sigma} \hat{a}_{i\sigma}^\dagger \hat{a}_{j\sigma} + U \sum_i \hat{n}_{i\uparrow} \hat{n}_{i\downarrow}, \quad (1)$$

where $\hat{a}_{i\sigma}$ is the usual Fermi creation operator ($\sigma = \uparrow, \downarrow$), $n_{i\sigma} = \hat{a}_{i\sigma}^\dagger \hat{a}_{i\sigma}$ the density, and $\langle ij \rangle$ denotes nearest neighbors. Only 2D square lattices at zero temperature will be studied here. U is the on-site usually repulsive interaction and t the nearest-neighbor hopping parameter. The model can be extended to include next-nearest-neighbor hopping (t') [7, 22] and longer-range hopping and interactions. We will mainly discuss the $t' = 0$ case where the phase diagram is symmetric around half filling. It is then sufficient to discuss only the doped case where $x = 1 - n \geq 0$.

As mentioned in the introduction, various approximations and numerical results to the Hubbard model lead to a variety of phases as ground state solutions. Long-range Coulomb repulsion present for the case of electrically charged electrons/holes further complicates the phase structure and will be included in a later section.

In the following two subsections two simple representative models, a MF and a stripe model, are investigated with and without PS respectively.

A. Phase Separation in Mean Field models

MF theory provides a first impression of the phases competing for the ground state and has the advantage that it is computationally simple as compared to more complicated theories. The MF equations for the Hubbard model are standard and we refer to, e.g., Refs. [7, 22]. The energy densities can be calculated within the Hartree-Fock approximation for the paramagnetic (PM), ferromagnetic (FM), antiferromagnetic (AF) and other

phases. In Fig. 1 we show an illustrative example for the energy density vs. filling fraction for $U = 6t$ and in the symmetric case $t' = 0$.

At low density $n \ll 1$ the ground state is that of a dilute paramagnetic (PM) gas with energy

$$\varepsilon_{PM} = -4tn + \left[\frac{\pi}{2}t + \frac{1}{4}U \right] n^2 + \mathcal{O}(n^3). \quad (2)$$

In units where the lattice spacing is unity ($a = 1$) this energy per site is also the energy density, and the density is the site filling fraction.

Near half filling $\varepsilon_{PM} = -(4/\pi)^2 t + U/4$, which becomes positive when the repulsive interaction exceeds $U/t \geq 64/\pi^2 \simeq 6.5$. The PM phase is then no longer the ground state. In a state with only one spin the antisymmetry of the wavefunction automatically removes double occupancy and the repulsive term $Un^2/4$ in Eq. (2) disappears. Such a ferromagnetic (FM) state always has negative energy $\varepsilon_{FM} \leq 0$ for $n \leq 1$ and is a candidate for the ground state. AF, linear AF [23] and stripe phases are other competing candidates.

For the 2D Hubbard model it is, however, necessary to extend MF to mixed phase scenarios. When $U \lesssim 7t$ the ground state of the MF Hubbard model undergoes transitions from an AF at half filling to a mixed AF+PM phase for $|x|$ up to a finite (U dependent) value whereafter a pure PM phase takes over. [7] For larger U the phase diagram is more complicated with a pure as well as mixed FM phases between the AF and PM phases. A finite next neighbor hopping term t' makes the phase diagram asymmetric around $x = 0$, extends the AF phase and changes the phase diagram considerably.

At half filling $n = 1$ the ground state is an AF. Near half filling $0 \leq x \ll 1$ the MF equations and AF energy can be expanded as

$$\varepsilon_{AF} = -J \left[1 + \frac{3}{2}x + 2x^2 + \dots \right]. \quad (3)$$

The concave dependence on x signals phase separation into a mixed phase of AF and PM by the Maxwell construction as shown in Fig. 1. The PS extends from the AF phase with density $n = 1$ to a PM phase with U dependent density $n_s = 1 - x_s \simeq 0.6$. The double tangent determines the PS energy ε_{PS} within MF.

The difference in energy between the PS and the PM/FM phases sets the energy and temperature scale for the AF correlations, which is related to the pseudogap, which in turn is related to the spin gap as [25] $T^* \sim \Delta_s/2$. We expect that the spin gap is of order the energy difference between the AF phase and spin uncorrelated PM or FM phase, whichever has lowest energy. Thus $T^* \sim (\varepsilon_{PS} - \varepsilon_{PM})/2 \sim (1 - x/x_s)J/2$. The AF spin correlations have a long but finite length scale so that the Mermin-Wagner theorem is not violated.

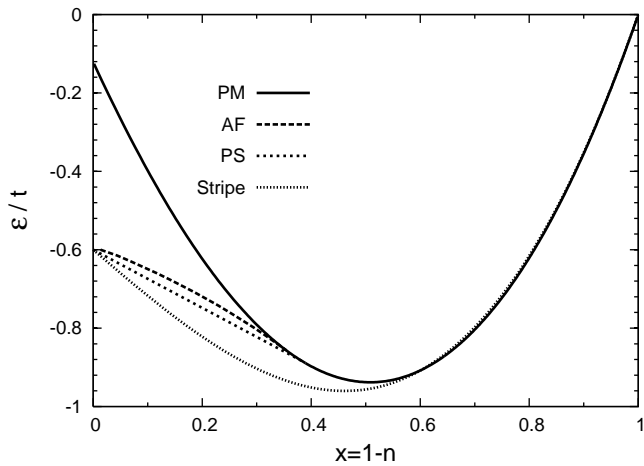


Figure 1: 2D Hubbard MF energy densities in the case $U = 6t$ are shown for the PM, AF and the Maxwell construction for the phase separation (PS). Also a stripe energy is shown (see text).

B. Stripe model

Stripes have been discovered in low-energy magnetic neutron scattering in doped cuprates at incommensurate longitudinal and horizontal charge and spin wave numbers [15], e.g. $\mathbf{Q}_c = (2\pi/a)(0, \pm x/x_s)$ and $\mathbf{Q}_s = (\pi/a)(1, 1 \pm x/x_s)$ for the longitudinal charge and spin wave numbers respectively. Here, the hole filling in the stripes is half filled $x_s = 1/2$ for low dopings $x \leq 1/8$ but at larger doping it increases linearly to filled stripes $x_s = 1$ such that $x/x_s = 1/4$ remains constant. Therefore the charge (spin) density stripes appear with periodic distance d ($2d$) depending on doping as $d = ax_s/x$. The stripe distance decreases with increasing doping until $x \geq 1/8$, whereafter the stripes remain at a distance $d = 4a$. The stripes act as anti-phase domain walls and the spin density wave therefore has periodicity twice the length of the charge-density wave.

Diagonal, horizontal/vertical, checkerboard stripe solutions have been found in a number of models. In MF models Zaanen and Gunnarson [13] found stripes of hole density $x_s = 1$ that are vertical or horizontal for $U/t \lesssim 3 - 4$ and diagonal otherwise. In DMRG calculations [14] stripes with hole density $x_s = 1/2$ are found in agreement with experiments [15].

Insight into pairing and stripe formation can be obtained by adding or removing one, two or more particles/holes in the half-filled AF. When the hole moves a distance of l lattice distances the kinetic energy is reduced by t/l^2 but the AF is frustrated by an energy $\sim lJ$. Solving such a simple linear string-like model for the one-hole problem in a 2D AF for $J \lesssim t$ leads to a hole localized within a distance $l \sim (t/J)^{1/3}$ with energy

$$\varepsilon_1 = -4t + \beta J^{2/3} t^{1/3}. \quad (4)$$

Within the WKB approximation one obtains $\beta =$

$(3\pi/4)^{2/3} \simeq 1.8$. Self consistent Born approximations [28] find similar hole energy $\varepsilon_1/t = -3.28 + 2.16(J/t)^{2/3}$ valid when $J \lesssim 0.4t$.

Because two nearby holes of opposite spin can move through the AF ordered lattice without upsetting the AF order they are not localized. If the pair has an energy that is lower than that of two separate holes $\varepsilon_2 > 2\varepsilon_1 - \varepsilon_0$, the odd-even difference can as in nuclear physics be taken as an effective pairing energy $\Delta = (\varepsilon_0 + \varepsilon_2)/2 - \varepsilon_1$.

Adding more holes one might expect that more pairs form, eventually creating a molecular Bose-Einstein condensate (mBEC) as in the BCS to BEC crossover in 3D ultracold atomic traps [26, 27]. On the square lattice such pairs have d-wave symmetry and mBEC will be a dSC [25]. However, a number of numerical calculations as well as experiments find that the holes form periodic stripes rather than forming a mBEC. The equi-distance of the stripes indicate that they “repel” each other even in calculations without Coulomb frustration. As a consequence the chemical potential must decrease with hole density or equivalently $\varepsilon'' \equiv (d^2\varepsilon/dx^2)_{x=0} > 0$, and we can expand the stripe energy density as

$$\varepsilon = -J - \varepsilon_1 x + \frac{1}{2}\varepsilon'' x^2 + \mathcal{O}(x^3), \quad (5)$$

for small doping. It is the second derivative ε'' of the energy density at small doping that distinguishes the phases. It is positive for the PM, FM and stripe phases, zero for PS but negative for the unstable AF.

The stripe phase is a specific ordered mixed AF and PM phase and is a continuous transition between the two pure phases as function of density. Similar mixed phase solutions are believed to occur in neutron star crusts between nuclear matter and a neutron gas [29], and possibly also between quark and nuclear matter [30]. In both cases Coulomb energies add complexity to the mixed phases by ordering them into structured crystallic phases.

III. COULOMB FRUSTRATION

Long range Coulomb interactions prevent phase separation into two bulk phases of different charge density. They also inhibit the formation of localized holes, pairs and stripes. The phase diagrams of cuprates with such Coulomb frustration and optical lattices without may therefore be very different.

Coulomb frustration in cuprates has been discussed in connection with stripes (see e.g. [25, 31]). Generally the CDW hole pairs and stripes are energetically less favorable due to long range Coulomb repulsion. In the following we shall consider the stripes as rods with charge less than the surrounding phase and calculate the additional Coulomb energy of such structures.

Coulomb energies have been calculated for structures of various dimensionality D and volume filling fraction f

[29]

$$\varepsilon_C = \frac{2\pi}{D+2} \Delta\rho^2 R^2 f \left[\frac{2}{D-2} \left(1 - \frac{D}{2} f^{1-2/D} \right) + f \right]. \quad (6)$$

Here, the charge density difference between the two phases is $\Delta\rho = ex_s/a^3$ for the stripes and the volume filling fraction is $f = x/x_s$. The filling fraction is also the inverse of the stripe distance in lattice units. The dimensionality is $D = 3$ for spherical droplets or bubbles, $D = 2$ for rods and tubes and $D = 1$ for plate-like structures. The diameter of the spheres, rods or the thickness of the plates is of order the distance between layers $2R \sim a \sim 4$. The stripes are rods in a 2D plane but are embedded in a 3D layered structure. For $D = 2$ the expression in the square bracket of Eq. (6) reduces to $[\ln(1/f) - 1 + f]$. The logarithm originates from the Coulomb integral $\int^l dz/z$ along the rod length z , which is cutoff by other rods at a length scale $l \sim a\sqrt{f}$. For the cuprates we furthermore reduce the Coulomb field by a dielectric constant of order $\epsilon \sim 5$. The resulting Coulomb energy of stripe or rod-like structures $D = 2$ is

$$\varepsilon_C \simeq \frac{\pi x_s e^2}{8 a^4 \epsilon} f [\ln(1/f) - 1 + f]. \quad (7)$$

Energy costs associated with the interface structures are usually added. Such surface energies are difficult to calculate for the stripes because their extent is only a single lattice constant. In principle they are already included in the stripe models. We will therefore just add the Coulomb energies given above. However, the Coulomb energies and the energy of the systems as a whole, may be reduced by screening and hole hopping into the AF whereby R increases but $\Delta\rho$ and f are reduced.

Inserting numbers $e^2/\hbar c = 1/137$, $\epsilon = 5$, $x_s = 1/2$, $a = 4$ we find that $\varepsilon_c \simeq 150 \text{ meV} x [\ln(1/f) - 1 + f]$. In comparison the energy gain by changing phase from an AF to a stripe or PM phase increases with doping as $(\varepsilon_{AF} - \varepsilon_{s/PM}) \sim \tilde{J}x$. The linear coefficient is $\tilde{J} = (\varepsilon_1 - 3J/2)$ for the stripe phase but considerably smaller for the PM phase $\tilde{J} \simeq 50 - 100 \text{ meV}$ according to Fig. 1. The Coulomb energy of Eq. (7) thus dominates at small doping due to the logarithmic singularity and therefore the AF phase of density $n \lesssim 1$ is preferred.

The AF phase is the ground state as long as the Coulomb energy of Eq. (7) exceeds $\tilde{J}x$ corresponding to doping less than

$$x_{AF} \simeq x_s \exp \left[-\frac{8 \tilde{J} a \epsilon}{\pi x_s e^2} - 1 \right]. \quad (8)$$

Inserting the above numbers and $\tilde{J} \simeq J$ we find $x_{AF} \simeq 0.1$ which is within range of the observed $|x_{AF}| \simeq 0.03$ for hole doped and $x_{AF} \simeq 0.15$ for particle doped cuprates. In MF the particle-hole asymmetry arises from the next-nearest neighbor hopping $t' \simeq -0.3t$ and leads to an AF phase extending from half filling up to a particle doped

density $n > 1$. [7] Note that it is not taken into account that with increasing doping the AF density approaches that of the PM, and eventually the charge difference $\Delta\rho$ between the AF and PM and the resulting Coulomb energy become sufficiently small that stripes are favored.

In the above picture the incommensurate stripe phases at small doping arise due to Coulomb frustration when $t' = 0$. At larger doping the stripes approach and will eventually affect each other. Experimentally the stripes undergo a transition from an incommensurate to a commensurate phase at $x \simeq 1/8$ corresponding to a stripe periodicity of four lattice spacings.

IV. SUPERFLUIDITY

Since phase separation and stripe phases are sensitive to Coulomb frustration, we can ask the related question: does superfluidity occur in 2D optical lattices with Fermi atom as in HTc cuprates or is Coulomb frustration required? The answer depends on the mechanism behind HTc which twenty years after its discovery is still not well understood. Like the ground state phases discussed above, the various models disagree about the origin of dSC and its dependence on the Hubbard parameters, doping and the influence of stripes and Coulomb frustration. In certain models [25], stripes are a prerequisite for dSC. In the following a simple semi-phenomenological model will be discussed based on similar ideas that pairing take place on stripes in an AF background.

Standard BCS superconductivity is s-wave and requires an attractive pairing interaction. HTc superconductivity is d-wave and is believed to arise in the correlated state of the Hubbard model with purely repulsive forces. The effective pairing must be a result of highly collective effects since the two-body interaction is strongly repulsive which inhibits onsite s-wave pairing but favors next-neighbor d-wave pairing between opposite spins due to super-exchange.

An instructive example where superfluidity arises is the 1D Hubbard model in a staggered or AF background magnetic field. At low magnetic field it is a normal metal as the standard 1D Hubbard model [32] whereas for strong field it becomes superfluid for $x \leq (2 - \sqrt{2})$ [33]. The staggered magnetic field leads to a linearly increasing string potential between holes of opposite spin and constitutes a strong effective pairing potential. However, the stripes observed in experiments have antiphase domain walls. The staggered magnetic field is therefore of opposite sign on the two sides of the stripe and no net staggering magnetic field results. No superconductivity is thus expected on the 1D stripes if detached from the surrounding 2D AF phase.

Instead, effective pairing correlations in two-leg ladder models are found transversely to the stripes [25]. Two features of superfluidity are important: that the electrons or atoms must pair and they must condense. These two features limit the critical temperature for weak

and strong pairing respectively. In the weak limit the critical temperature is exponentially suppressed as in standard BCS $T_c \sim \exp(-1/g)$ (for 2D see Eq. (13)), where g is the product of the pairing attraction and the level density. In the strong limit it is argued [25] that $T_c = \hbar^2 n_s(T=0)/4m^*$ where n_s is the superfluid density and m^* the effective mass of the particle. The superfluid density is limited by the density of holes and thus vanishes with decreasing doping.

A simple model will now be constructed that incorporates these ideas for the inhomogeneous stripe phase in a semi-phenomenological way. The weakly interacting limit, where the effective pairing and T_c vanish, is approached when the AF correlations dissolve and the PM phase appears. To estimate the pairing in this BCS limit we assume for simplicity that the pairing take place between nearest neighbor holes and, since it is driven by the AF correlations, that its effective strength V is proportional to the volume of the AF. Specifically, we shall assume that it vanishes when there is only one AF stripe between each half filled stripe, i.e.

$$V = V_0(1 - 2x/x_s). \quad (9)$$

Here, the effective pairing strength must exceed $V_0 \geq 2t$ and $V_0 \gtrsim 7.35t$ in order that holes can form s-wave and d-wave two-body bound states respectively [34]. In contrast the onset of superconductivity occurs for $V_0 > 2t$ and $V_0 > 0$ respectively.

In the strongly interacting limit at low hole density we ensure that the superfluid density vanishes with hole density by explicitly multiplying the density of states by the hole density.

Generally, we assume the pairing takes place between pairs in the stripes, although pairs can tunnel between stripes. The derivation of the gap equation for holes then follows that of standard BCS on a lattice (see e.g. [22]). The pairing is expected to be d-wave with a gap $\Delta_{\mathbf{q}} = 2\Delta[\cos(q_x) - \cos(q_y)]$ since s-wave is suppressed by on-site repulsion [22, 34]. The resulting dSC gap equation for the critical temperature T_c is

$$\frac{1}{V} = \frac{x}{x_s} \frac{1}{N} \sum_{\mathbf{q}} [\cos(q_x) - \cos(q_y)]^2 \frac{\tanh(\bar{\epsilon}_{\mathbf{q}}/2T_c)}{2\bar{\epsilon}_{\mathbf{q}}}. \quad (10)$$

Here, it should be noted that the prefactor x/x_s ensures that the level density sums up to the correct hole density on the stripes. The chemical potential is determined by the hole density in the stripes

$$x_s = \frac{1}{N} \sum_{\mathbf{q}} \tanh(\bar{\epsilon}_{\mathbf{q}}/2T). \quad (11)$$

For simplicity we assume that the holes act as free electrons on the lattice with dispersion $\bar{\epsilon}_{\mathbf{q}} = -2t[\cos(q_x) + \cos(q_y)] - \mu$.

For large critical temperature $T_c \gtrsim t$ the integral on the r.h.s. of the gap equation is simple and we obtain $T_c = Vx/4x_s = V_0(1 - 2x/x_s)x/4x_s$. The pairing strength

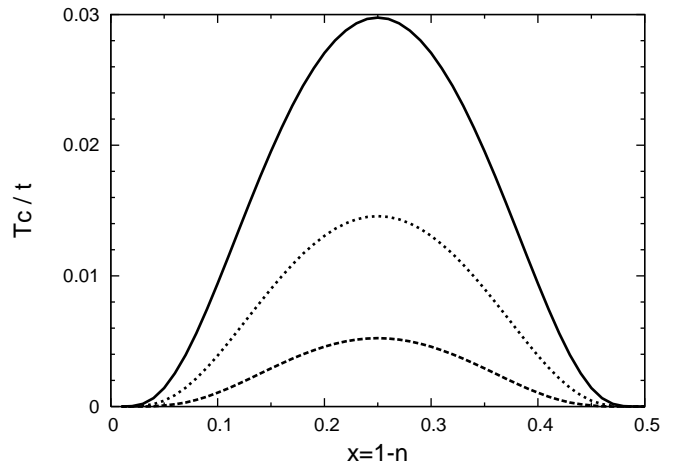


Figure 2: Critical temperature vs. doping from Eq. (13) for $V_0/t = 2, 3, 4$ from bottom and up, and $x_s = 1$.

is, however, not strong enough to satisfy that condition. For small critical temperature and $x_s \simeq 1$ ($\mu = 0$) the singularities at $\bar{\epsilon}_{\mathbf{q}} = 0$ allows us to calculate the gap integral to leading logarithmic orders

$$\frac{t}{V} = \frac{1}{\pi^2} \frac{x}{x_s} [\ln^2(2t/T_c) + 0.4 \ln(2t/T_c) + 1.78]. \quad (12)$$

Besides the usual BCS log originating from the energy denominator another log arises from the logarithmic level density due to the van Hove singularity in a 2D lattice at half filling. The resulting critical temperature from Eq. (12) is

$$T_c = 2t \exp \left[-\sqrt{\pi^2 t x_s / (xV)} - 1.74 + 0.2 \right]. \quad (13)$$

The filled stripe condition $x_s \simeq 1$ is, however, only valid for dopings $1/4 \lesssim x \lesssim 1/2$. For lower doping the filling is smaller, e.g. $x_s \simeq 0.5$ for $x \leq 1/8$. The lower density of holes generally reduces T_c [22].

The stripe superfluidity differs from a superfluid of hole pairs. The latter phase would be similar to the molecular Bose-Einstein condensate (mBEC) discovered in ultracold atomic 3D traps (without lattices) when a dilute gas of attractive fermionic atoms cross the unitarity limit (infinite scattering length) and cross over from a BCS to a mBEC [26]. The critical temperature for the superfluid mBEC is of the order of the Fermi energy in 3D $T_c = \hbar^2 (n/2\zeta(3/2))^{2/3} \pi/m \simeq 0.218 E_F$ in the mBEC and slightly larger in the unitarity limit [35]. In 2D, however, the critical temperature for a BEC vanishes and can therefore not explain HTc.

In Fig. 2 the critical temperatures for dSC of Eq. (13) is shown for three effective pairing interactions. By construction d-wave superfluidity vanishes near $x \sim 1/2$, where the effective pairing V vanishes, and also as $x \rightarrow 0$, where the density of holes disappears. Thus the simple stripe pairing model gives a qualitative description of HTc. In contrast d-wave superfluidity is largest at

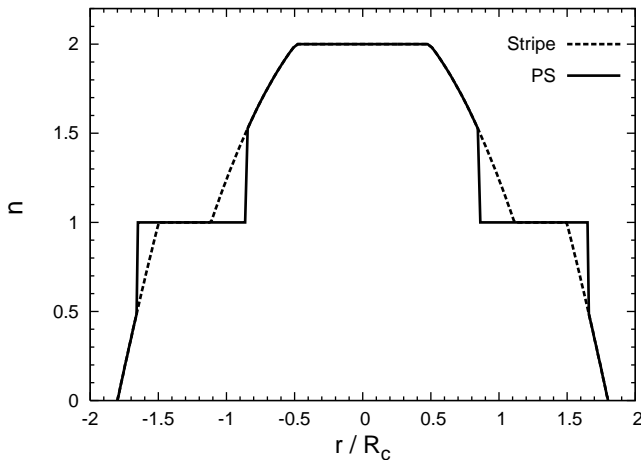


Figure 3: Density distributions of Fermi atoms in an optical lattice confined by a harmonic trap. $U = \langle \epsilon'' \rangle = 6t$ and $x_s = 1/2$. Full (dashed) curves represents the PS (stripe) equation of states (see text).

low doping for standard uniform Hubbard models with an attractive interaction and it extends to large doping. [22, 37]

As discussed above the semi-phenomenological stripe dSC model is just one of many models for HTc dSC. It has the interesting consequence that if PS occurs in optical lattices there will be no stripes and therefore no dSC either. Both will have direct observational consequences in optical lattices.

V. OPTICAL LATTICES IN TRAPS

We can now address the phases present in optical lattices based on the equation of states for the 2D Hubbard model without Coulomb frustration, and calculate quantities measured experimentally.

In the limit of many particles in a shallow confining potential, the Thomas-Fermi approximation (TF) applies because the length scales over which the trapping potential and density varies are long compared to phase boundaries and the lattice spacing [36]. We shall in the following assume that the confining potential is on a harmonic oscillator form $V_2 r^2$ as is the case in most experiments. Within TF the total chemical potential is given by the sum of the trap potential and the local chemical potential $\mu(n) = d\varepsilon/dn$, where ε and $n(r)$ are the local energy and number density per site respectively, i.e.

$$\mu_{Tot} = \mu(n) + V_2 r^2 = \mu(n=0) + V_2 R^2. \quad (14)$$

It must be constant over the lattice and can therefore be set to its value at the edge or radius R of occupied lattice sites, which gives the last equation in (14). The chemical potential for the dilute lattice gas in the 2D Hubbard model is $\mu(n=0) = -4t$.

Measuring the density distribution $n(r)$ gives the chemical potential by inverting Eq. (14), and the equation of state can therefore be determined experimentally. We can from the above estimates for the equation of states also predict the density distribution at least qualitatively. The scale of the chemical potential is rather limited since it only varies from $\mu(0) = -4t$ in the dilute limit to a value at half filling between zero for the weakly repulsive PM ($U \ll t$) and $\mu(1) = 4t$ for the FM in the strongly repulsive limit ($U \gg t$). Near half filling the chemical potential is $\mu(n=1) = \epsilon_1$ for the stripe model. For the PS model the chemical potential is smaller and constant between $0 < x < x_s$, yet on a similar scale $\mu(n=1) \sim 2t$. The average slope of the chemical potential is therefore $\langle \epsilon'' \rangle = \mu(n=1) - \mu(n=0) \sim 6t$. Approximating the chemical potential with such a linear density dependence $\mu = \langle \epsilon'' \rangle n$ we obtain for $n \leq 1$

$$n(r) = \frac{V_2}{\langle \epsilon'' \rangle} (R^2 - r^2). \quad (15)$$

The PM and stripe phases below half filling therefore extends up to a radius $R_c = \sqrt{\varepsilon''/V_2}$. The chemical potential $\mu(n)$ has a gap at half filling which is of order U . As result a Mott insulator or AF density plateau appears at $n = 1$, which extends a radial distance of order $\sim \sqrt{U/V_2}$. The phases repeat for densities above half filling up to the band insulator at $n = 2$ such that the characteristic “wedding cake layers” appear as shown in Fig. 3. The stripe and PS models differ qualitatively at densities around half filling where the latter has a discontinuity at $n = n_s$ and $n = 2 - n_s$, where we expect $n_s \simeq 0.5$ as discussed above. The stripe phase is a d-wave superfluid between the AF and PM phases whereas no such intermediate superfluid appears for the PS model. In both cases the AF phase is a MI at half filling $n = 1$ only, whereas in the cuprates the AF extends between densities 0.95 – 1.2 due to Coulomb frustration or possibly a finite t' . Detailed measurements of the densities in confined optical lattices near half filling could therefore in principle reveal the effects of Coulomb frustration.

The density and radius are related through (14) and the corresponding total number of atoms in the confined lattice is

$$N = \frac{2\pi}{a^2} \int_0^R n(r) r dr. \quad (16)$$

The critical numbers for the stripe and AF/MI phases to appear in the center of the trap are $N = \pi R_c^2/4a^2$ and $N = \pi R_c^2/2a^2$ respectively. Fillings above half filling $n = 1$ and up to the band insulator BI $n = 2$ can be reached by adding more atoms as shown in Fig. 3. The critical fillings and radii depend on the ratio of $U/\langle \epsilon'' \rangle$. For $U \gg \langle \epsilon'' \rangle$ the MI plateau dominates the density distribution and the number of particles required to reach higher densities and the BI in the center is $N = \pi U/V_2 a^2$.

Other possible scenarios are qualitative different. If HTc is described by the 2D Hubbard model without

Coulomb frustration, then we can expect that the MI is replaced by an AF phase around $n = 1$ surrounded by two dSC phases at densities lower (hole doped) and higher (particle doped). According to [9] phases with AF and dSC order are mixed when $U \lesssim 8t$ but coexist when $U \gtrsim 8t$ with a first order transition between two densities. A critical point is predicted where a mixed AF+dSC phase terminate and is replaced by a first order phase transition. Here the AFM and dSC phases are separated and coexist with a density discontinuity. In [11], however, the pure dSC undergo a first order transition to a mixed AF+dSC phase. The densities at which these transitions take place correspond to doping $x \simeq \pm 0.1$. If nearest neighbor interactions or next-nearest neighbor hopping are included, the particle-hole symmetry is broken and the phase diagram becomes asymmetric around half filling ($n = 1$). The models differ dramatically in their predictions of the phases in the shells surrounding the MI shell.

Experimentally the density distributions and shell structures have been measured for Bose atoms in optical lattices by a slicing method in combination with microwave transitions that differentiates between singly and doubly occupied sites. [2] Very low temperatures and fine resolution will be required in order to observe the density discontinuities of Fig. (3).

The momentum distributions of atoms in the confined lattice can be found by time of flight experiments. After the system has expanded a time t the column integrated densities are measured by light absorption imaging. In such time of flight experiments the position is related to the momentum in the lattice before free expansion as $\mathbf{r} = \mathbf{k}t/m$ in the far field approximation. As a result one measures the momentum distribution $\langle n_{\mathbf{k}} \rangle$ and correlations $\langle n_{\mathbf{k}} n_{\mathbf{k}'} \rangle$ of atoms in confined lattice. In a sudden release $\langle n_{\mathbf{k}} \rangle$ is dominated by the Fourier transform of the tight binding Wannier functions in the case of Fermi atoms whereas a BEC displays characteristic Bragg peaks. However, by adiabatically turning off the optical lattice potential with Fermi atoms only the crystal momenta in the lowest Bloch band remains, which for a 2D band insulator is a square $|k_{x,y}| \leq \pi$, as observed in [5]. If the adiabatic release can be made perfect at very low temperatures it is in principle possible to measure accurate momentum distributions. In a AF+PM mixed phase one should observe a two-component momentum distribution: a square from the MI and a circular on top from the PM. This also requires on-site repulsive interaction which must be turned off suddenly or corrected for in the expansion.

The density-density correlation function is

$$\langle \hat{n}_{\mathbf{k}} \hat{n}_{\mathbf{k}'} \rangle = \delta_{\mathbf{k}\mathbf{k}'} \langle \hat{n}_{\mathbf{k}} \rangle + \langle \hat{a}_{\mathbf{k}} \hat{a}_{\mathbf{k}'} \hat{a}_{\mathbf{k}}^\dagger \hat{a}_{\mathbf{k}'}^\dagger \rangle, \quad (17)$$

where the first term is the auto-correlations which is suppressed by a factor $1/N$ and can therefore be ignored. We proceed by expanding the field operator in terms of Wannier functions: $\hat{a}(\mathbf{k}) = w(\mathbf{k}) \sum_{\mathbf{R}} e^{-i\mathbf{k}\mathbf{R}} \hat{a}(\mathbf{R})$, over the Bravais lattice \mathbf{R} . We assume factorization into one-

particle density matrices $\langle \hat{a}(\mathbf{R}) \hat{a}(\mathbf{R}') \rangle = n_{\mathbf{R}} \delta_{\mathbf{R}\mathbf{R}'}$ [39] which, however, excludes off-diagonal orders from phase coherence in a superfluid. Superfluids will be discussed later. In non-superfluid systems we then obtain the correlation function

$$\begin{aligned} C(\mathbf{k}, \mathbf{k}') &= \frac{\langle \hat{n}_{\mathbf{k}} \hat{n}_{\mathbf{k}'} \rangle}{\langle \hat{n}_{\mathbf{k}} \rangle \langle \hat{n}_{\mathbf{k}'} \rangle} \\ &= 1 - \frac{1}{N^2} \sum_{\sigma} \left| \sum_{\mathbf{R}} e^{i(\mathbf{k}-\mathbf{k}')\mathbf{R}} n_{\mathbf{R}\sigma} \right|^2, \quad (18) \end{aligned}$$

with $\langle \hat{n}_{\mathbf{k}} \rangle = N|w(\mathbf{k})|^2$. For bosons the minus sign is replaced by a positive one and gives the characteristic Hanbury-Brown & Twiss bunching observed for photons in stellar interferometry and for mesons in relativistic heavy ion collisions [40]. For non-interacting Fermi atoms the minus sign simply enforces the Pauli principle which inhibits two atoms occupying the same momentum state.

For MI and BI phases of bosons and fermions the occupation numbers $n_{\mathbf{R}}$ are numbers, and the sum in Eq. (18) yields Bragg peaks and dips respectively whenever the momentum difference equals the reciprocal lattice vectors, i.e. $\mathbf{q} = \mathbf{k} - \mathbf{k}' = 2\pi(n_x, n_y)$, where $n_{x,y}$ are integers and in units $a = 1$. The radius of the occupied sites in the optical lattice limits the sum in Eq. (18) and results in a finite momentum width of the peaks and dips of order the inverse radius.

Bragg peaks have been observed for bosons in 3D [2] and 2D [4] lattices, and dips for 3D fermions in [6]. The Bragg peaks and dips occur in $C(\mathbf{k}, \mathbf{k}')$ when $\mathbf{q} = \pi(n_x, n_y)$, where n_x, n_y are even integers. In an AF phase the periodicity of a given spin is two lattice distances and anti-bunching also appears for odd integers by an amount [37] $C(\mathbf{k}, -\mathbf{k}) = [(Um/2)/2E_{\mathbf{k}}]^2$, where m is the AF order parameter and $E_{\mathbf{k}} = \sqrt{(Um/2)^2 + \bar{\epsilon}_{\mathbf{k}}^2}$ the quasiparticle energy.

Just as for the AF phase we can in a stripe phase expect charge and spin correlations as in low energy magnetic neutron scattering, i.e. $\mathbf{q} = \mathbf{Q}_c$ and $\mathbf{q} = \mathbf{Q}_s$ respectively, observed as anti-bunching at these wave-numbers. However, because the doping x varies in the confined optical lattice, the Bragg dips are distributed over the range of values for x/x_s and are therefore hard to distinguish from the background. If, however, the four stripe periodicity with $x/x_s = 1/8$ occurs for $1/8 \leq x \leq 1/4$ as in HTc, we can expect novel Bragg dips for charge correlations at $\mathbf{q} = (0, \pm\pi/2)$ and $\mathbf{q} = (\pm\pi/2, 0)$ and for spin correlations at $\mathbf{q} = \pi(1, 1 \pm 1/4)$ and $\mathbf{q} = \pi(1 \pm 1/4, 1)$.

Pairing occurs between opposite momenta and leads to bunching for $\mathbf{k} = -\mathbf{k}'$. Recently, phase coherence and s-wave pairing has been observed in optical lattices with attractive onsite interactions near the BCS-BEC crossover [3]. As the lattice heights are increased the MI phase dominates and phase coherence is gradually lost. For repulsive on-site interactions the weaker d-wave superfluidity may appear as discussed above. We can expect atoms bunching by the amount [37] $C(\mathbf{k}, -\mathbf{k}) = \Delta_{\mathbf{k}}^2/2E_{\mathbf{k}}^2$, where the quasiparticle energy is $E_{\mathbf{k}} = \sqrt{\Delta_{\mathbf{k}}^2 + \bar{\epsilon}_{\mathbf{k}}^2}$. If dSC is

associated with stripes, the bunching due to d-wave superfluidity should occur in conjunction with the stripe anti-bunching.

VI. SUMMARY

In conclusion, ultracold fermionic atoms in confined optical lattices can reveal details of the equation of state and phases of the 2D Hubbard model for a variety of interaction and hopping parameters. Specifically two plausible models have been investigated with phase separation and stripe formation respectively that results in qualitatively different density distributions in optical lattices with and without density discontinuities. However, in the cuprates Coulomb frustration can induce stripe formation in both cases which makes it hard to distinguish between the two cases. Coulomb frustration could as shown in a simple model also be responsible for an antiferromagnetic phases extending from densities be-

tween 0.95 – 1.15 in cuprates whereas in optical lattices only $n = 1$ MI plateau should form because there is no Coulomb frustration. If stripes are required for high temperature superconductivity, one will not observe superfluidity in optical lattices if phase separation occurs.

We conclude that the various PM, FM, AF, d-wave superfluidity and possibly also stripe phases can be observed by measurements of densities, momentum distributions and correlations in expanding ultracold atoms from optical lattices. Bunching and anti-bunching correlations can reveal these phases at characteristic Bragg momenta. By varying the filling densities, interaction strengths and temperatures, the onset and amount of the various phases can be studied in order to determine the equation of states. Experimental determination of AF, stripe, metal and/or d-wave superfluid phases will severely restrict the models, and the density and temperature dependence on parameters such as U, t, t' will provide much understanding of the Hubbard model and HTc.

-
- [1] T. Stöferle *et al.*, Phys. Rev. Lett. **96**, 030401 (2006).
 - [2] S. Fölling *et al.*, Nature **434**, 481 (2005).
 - [3] J.K. Chin, D. E. Miller, Y. Liu, C. Stan, W. Setiawan, C. Sanner, K. Xu, W. Ketterle, Nature **443**, 961 (2006).
 - [4] I.B. Spielman, W.D. Phillips, and J.V. Porto, Phys. Rev. Lett. **98**, 080404 (2007).
 - [5] M. Köhl *et al.*, Phys. Rev. Lett. **94**, 080403 (2005).
 - [6] T. Rom, Th. Best, D. van Oosten, U. Schneider, S. Foelling, B. Paredes, I. Bloch, Nature **444**, 733 (2006).
 - [7] E. Langmann and M. Wallin, cond-mat/0406608.
 - [8] A. Moreo, D. Scalapino, and E. Dagotto, Phys. Rev. B **43**, 11442 (1991).
 - [9] F. Becca, M. Capone and S. Sorella, Phys. Rev. B **62**, 12700 (2000).
 - [10] R. Zitzler, Th. Pruschke, and R. Bulla, Eur. Phys. J. B **27**, 473 (2002).
 - [11] M. Aichhorn and E. Arrigoni, Europhys. Lett. **71**, 117 (2005).
 - [12] A. Macridin, M. Jarrell and Th. Maier, Phys. Rev. B **74**, 085104 (2006).
 - [13] J. Zaanen and O. Gunnarsson, Phys. Rev. B **40**, 7391 (1989). D. Poilblanc and T.M. Rice, Phys. Rev. B **39**, 9749 (1989). H.J. Schulz, J. Physique, **50**, 2833 (1989); K. Machida, Physica C **158**, 192 (1989).
 - [14] D.J. Scalapino, Physics Reports **250**, 329 (1995); and cond-mat/0610710, to appear as Chapter 13 in "Handbook of High Temperature Superconductivity", J. R. Schrieffer, editor, Springer, 2006. S.R. White and D.J. Scalapino, Phys. Rev. Lett. **81**, 3227 (1998).
 - [15] J.M. Tranquada *et al.*, Phys. Rev. B **54**, 7489 (1996).
 - [16] S. Sorella *et al.*, Phys. Rev. Lett. **88**, 117002 (2002).
 - [17] M. Capone and G. Kotliar, Phys. Rev. B **74**, 054513 (2006).
 - [18] M. Aichhorn, E. Arrigoni, M. Potthoff, and W. Hanke, Phys. Rev. B **74**, 024508 (2006).
 - [19] W. Hofstetter *et al.*, Phys. Rev. Lett. **89**, 220407 (2002).
 - [20] V.J. Emery and S.A. Kivelson, Physica C **209**, 597 (1993).
 - [21] J. Hubbard, Phys. Rev. B **17**, 494 (1978).
 - [22] R. Micnas, J. Ranninger, S. Robaszkiewicz and S. Tabor, Phys. Rev. B **37**, 9410 (1988).
 - [23] C. Kusko and R.S. Markiewicz, cond-mat/0102440.
 - [24] T. Aima and M. Imada, J. Phys. Soc. Jpn. **76**, 113708 (2007).
 - [25] E. Arrigoni, E. Fradkin and S.A. Kivelson, Phys. Rev. B **69**, 214519 (2004).
 - [26] A.J. Leggett, in *Modern Trends in the Theory of Condensed Matter*, ed. A. Pekalski and R. Przystawa, Lect. Notes in Physics Vol. **115** (Springer-Verlag, 1980), p. 13.
 - [27] C. Chien, Y. He, Q. Chen and K. Levin, cond-mat/07063417.
 - [28] P.A. Lee, N. Nagaosa, and X-G. Wen, Rev. Mod. Phys. **78**, 17 (2006).
 - [29] C.P. Lorenz, D.G. Ravenhall and C.J. Pethick, Phys. Rev. Lett. **70**, 379 (1993)
 - [30] H. Heiselberg, C. J. Pethick and E. F. Staubo, Phys. Rev. Lett. **70**, 1355 (1993).
 - [31] G. Seibold, C. Castellani, C. Di Castro, and M. Grilli, cond-mat/9803184 J. Lorenzana, C. Castellani, C. Di Castro, Phys. Rev. B **64**, 235128 (2001).
 - [32] E.H. Lieb and F.Y. Wu, Phys. Rev. Lett. **20**, 1445 (1968).
 - [33] C.D. Batista and G. Ortiz, Phys. Rev. Lett. **85**, 4755 (2000).
 - [34] F. Pistolesi and Ph. Nozieres, Phys. Rev. B **66**, 054501 (2002).
 - [35] J. Kinast *et al.*, Science **307**, 1296 (2005).
 - [36] H. Heiselberg, Phys. Rev. A **74**, 033608 (2006).
 - [37] B.M. Andersen and G.M. Bruun, Phys. Rev. A **76**, 041602(R) (2007)
 - [38] E. Altman, E. Demler, and M.D. Lukin, Phys. Rev. A **70**, 013603 (2004)
 - [39] I. Bloch, J. Dalibard, and W. Zwerger, cond-mat/0704.3011. To appear in Rev. Mod. Phys.
 - [40] G.A. Baym, Act. Phys. Pol. B **29**, 1839 (1998).